



Published in final edited form as:

*Osteoarthritis Cartilage*. 2008 October ; 16(10): 1150–1159. doi:10.1016/j.joca.2008.02.018.

## Relationship between trabecular bone structure and articular cartilage morphology and relaxation times in early OA of the knee joint using parallel MRI at 3T

Radu I. Bolbos<sup>1</sup>, Jin Zuo<sup>1</sup>, Suchandrima Banerjee<sup>1,2</sup>, Thomas M. Link<sup>1</sup>, C. Benjamin Ma<sup>3</sup>, Xiaojuan Li<sup>1</sup>, and Sharmila Majumdar<sup>1,2</sup>

<sup>1</sup>Musculoskeletal Quantitative Imaging Research, Department of Radiology, University of California San Francisco, San Francisco, CA, USA

<sup>2</sup>Joint Graduate Group in Bioengineering, University of California Berkeley, Berkeley, CA, USA

<sup>3</sup>Department of Orthopaedic Surgery, University of California San Francisco, San Francisco, CA, USA

### Abstract

**Objective**—To evaluate trabecular bone structure in relationship with cartilage parameters in distal femur and proximal tibia of the human knee at 3 Tesla (3T) using high-resolution magnetic resonance imaging (MRI) with parallel imaging.

**Method**—Sixteen healthy controls and sixteen patients with mild OA were studied using a 3T MR scanner and an 8 channel phase-array knee coil. Axial 3D Generalized Autocalibrating Partially Parallel Acquisition (GRAPPA) – based phase cycled Fast Imaging Employing Steady State Acquisition (FIESTA-c) images were acquired in order to quantify the trabecular bone structure. For assessing cartilage morphology (thickness, volume), sagittal high-resolution 3D spoiled gradient echo (SPGR) images were acquired. In a subset of the subjects, sagittal images were acquired for measuring T1ρ and T2 relaxation times, using 3D T1ρ and T2 mapping techniques.

**Results**—Good measurement reproducibility was observed for bone parameters, the CVs ranging from 1.8% for trabecular number (app. Tb.N) to 5.5% for trabecular separation (app. Tb.Sp). Significant differences between control and OA groups were found for bone volume fraction (app. BV/TV) and app. Tb.Sp in all compartments. Significantly increased values in T1ρ and T2 were demonstrated in OA patients compared with controls at the femur, but not at the tibia. T1ρ was negatively correlated with app. BV/TV, app. Tb.N and app. Tb.Sp both at the medial femoral condyle (MFC) and lateral tibia (LT), while T2 was only correlated at the LT. Also, medial tibia (MT) T1ρ was negatively correlated with app. BV/TV ( $R^2 = -0.49$ ,  $P < 0.05$ ) and app. Tb.N ( $R^2 = -0.42$ ,  $P < 0.05$ ) from the opposite side of lateral femoral condyle (LFC). Significant correlations were found between trabecular bone parameters and cartilage thickness and normalized volume, mainly at LT, tibia (T) and femur (F).

**Conclusion**—At this early stage of OA, an overall decrease in bone structure parameters and an increase in cartilage parameters (T1ρ, T2) were noticed in patients. Trabecular bone structure

---

Corresponding Author: Radu I. Bolbos, PhD, 185 Berry Street, Suite 350, Department of Radiology, University of California at San Francisco, San Francisco, CA 94107, Tel: (415) 353-4928, Fax: (415) 353-3438, E-mail: radu.bolbos@radiology.ucsf.edu.

**Publisher's Disclaimer:** This is a PDF file of an unedited manuscript that has been accepted for publication. As a service to our customers we are providing this early version of the manuscript. The manuscript will undergo copyediting, typesetting, and review of the resulting proof before it is published in its final citable form. Please note that during the production process errors may be discovered which could affect the content, and all legal disclaimers that apply to the journal pertain.

correlated with articular cartilage parameters suggesting that loss of mineralized bone is associated with cartilage degeneration.

### Keywords

osteoarthritis; trabecular bone; cartilage; Magnetic Resonance Imaging; T1 $\rho$ ; T2

## INTRODUCTION

Osteoarthritis (OA) is a degenerative joint disease which typically affects the weight-bearing knee joints. It was suggested that pathological alterations at early stage of OA primarily affect the articular cartilage and the underlying bone<sup>1–3</sup>. The articular cartilage's early changes consist in increase in water content, loss of proteoglycans (PGs) and disruption of collagen fibers<sup>4</sup>, while for trabecular bone, the volumetric mineral density decreases due to incomplete mineralization of trabecular structure<sup>5</sup>. As the early OA stages are practically asymptomatic, the need of an early detection method is necessary.

Quantitative magnetic resonance imaging (qMRI) could serve as an early marker of changes in the mechanical properties of cartilage and underlying bone. qMRI provides a way to directly assess the integrity (thickness and volume) and composition (T1 $\rho$ , T2) of the articular cartilage *in vivo* in osteoarthritis. Eckstein et al.<sup>6</sup> evaluated the precision of qMRI when performed on 1.5T and 3T magnets, reporting errors from 1 to 4% for cartilage thickness and volume measurements. In the last years, significant interest focused on imaging cartilage biochemical composition. In particular, T1 $\rho$  and T2 relaxation time mapping techniques have been proposed to quantitatively examine the early stages of cartilage degeneration. T2 mapping represents a significant marker of cartilage degeneration by its sensitivity to tissue hydration and biochemical composition related to the integrity of collagen in the cartilage extracellular matrix<sup>7–9</sup>. Quantitative T1 $\rho$  mapping based on spin-locking technique represents a potential of MRI to reflect changes in biochemical composition of cartilage with early OA, such as proteoglycan loss<sup>10–13</sup>. These studies demonstrated that the higher the values of these relaxation parameters, the more significant changes take place within the cartilage organization (collagen fibers) and composition (proteoglycan). Li et al.<sup>14</sup> quantified the cartilage volume and thickness as well as T1 $\rho$  and T2 values at 3T and compared these parameters between normal and OA patients. They found that the average T1 $\rho$  and T2 values were significantly increased in OA patients compared with controls, whereas no significant difference was found in terms of cartilage volume and thickness. They suggested that, based on these significantly higher values of the T1 $\rho$  and T2 relaxation times obtained in patients, early degeneration could take place within the cartilage composition before the morphological changes occur.

Remarkable progress in high-resolution MRI (HR-MRI) over the last 15 years offers now a new promising noninvasive tool for depicting trabecular microstructure *in vivo*<sup>15, 16</sup>. Trabecular bone consists of a network of oriented elements or trabeculae (~80–100  $\mu\text{m}$ ) that are usually spaced ~200  $\mu\text{m}$  apart. Given the size of the trabeculae, spatial resolution is perhaps the single most critical parameter since this is required to be in the order of the trabeculae structural dimension for an accurate representation of topology, scale and orientation of trabecular bone networks. Since spatial resolution and signal-to-noise ratio (SNR) are inversely related, imaging at even higher spatial resolutions would entail a very long acquisition time to maintain a reasonable SNR. The currently achievable spatial resolution for *in vivo* trabecular bone imaging is ~130–190  $\mu\text{m}$  in plane and ~500  $\mu\text{m}$  through plane with an acquisition time of 15–20 minutes<sup>17, 18</sup>.

Several qMRI techniques have recently been introduced for the noninvasive assessment of structure and composition of trabecular bone and articular cartilage. An *ex vivo* study

investigated human cadaver patellae employing qMRI and several reference methods, demonstrating the relationship between structural and mechanical properties of articular cartilage and trabecular bone with different stages of degeneration<sup>19</sup>. Beuf et al.<sup>1</sup> performed an *in vivo* MRI study and demonstrate significant variations in trabecular bone structure within the knee joint in patients with OA. Other previous studies using the same *in vivo* MRI technique<sup>2, 3</sup> demonstrated that cartilage degeneration in the knee joint is associated with changes in trabecular bone structure, and that cartilage loss on one side of the knee joint is related to loss of mineralized trabecular bone on the opposite side of the knee joint.

Over the last few years, parallel MRI acquisition strategies have been proposed and have seen increased acceptance in the MRI community. In parallel MRI, spatial information contained in the component coils of an array is used to partially replace spatial encoding normally performed by gradients, thereby reducing imaging time<sup>20-22</sup>. One of them, Generalized Autocalibrating Partially Parallel Acquisitions (GRAPPA) technique is particularly suitable for small field-of-view imaging<sup>22</sup>. Structural depiction of trabecular bone has been seen to be preserved in images in GRAPPA based parallel MRI. In this work, we apply GRAPPA based parallel MRI method to shorten the acquisition time involved in high resolution MRI of trabecular bone, thereby reducing patient motion induced artifacts. The time saved can also allow more flexibility in the protocol design.

Therefore, the aim of this study is to use high-resolution magnetic resonance imaging (MRI) to evaluate the trabecular bone structure in the distal femur and the proximal tibia and to establish its relationship with articular cartilage of the human knee at 3T strength field using a parallel imaging protocol.

## MATERIAL AND METHODS

### Subjects

The study was performed in accordance with the rules and regulations the Committee for Human Research at our institution. Informed consent was obtained from all of the subjects after the nature of the examinations had been fully explained. An orthopedic surgeon recruited all subjects based on clinical investigation and diagnosis from antero-posterior weight-bearing radiographs. The severity of each subject's OA was evaluated based using the X-ray based Kellgren-Lawrence scale<sup>23</sup>.

Sixteen normal control subjects who did not show any clinical symptoms of OA (7 female, 9 male, age range 27 to 56 years; average = 36.3 years) were recruited and classified as Control group. Sixteen patients (7 female, 9 male, age range 29 to 72 years; average = 47.2 years) which exhibited mild radiographic signs of OA (K-L grades of 1 or 2) were classified as mild OA Group. A standardized questionnaire (Western Ontario and McMaster Universities Pain, Stiffness, and Physical Function scales, WOMAC)<sup>24</sup> for measuring the degree of pain, functional impairment and stiffness in all subjects through a 5-point scale (none, slight, moderate, severe and extreme) was used. The subject characteristics are presented in Table 1. Reproducibility of the trabecular bone structure measurements was assessed in 4 healthy controls (4 male, age = 31 – 39 years) with repositioning between 2 measurements.

### MRI protocol

MRI of the study knee of each subject was acquired at a 3T GE Excite Signa MR scanner (General Electric, Milwaukee, WI) using an 8 channel phased-array knee coil (General Electric Medical Systems, WI).

**Morphologic imaging**—In order to quantify the trabecular bone structure, images were acquired with axial fully refocused steady-state free-precession (SSFP) 3D phase cycled Fast Imaging Employing Steady State Acquisition (3D FIESTA-c) sequence. The sequence parameters were: TR/TE = 11/4.2 ms, acquisition matrix =  $512 \times 384$ , flip angle =  $60^\circ$ , field of view (FOV) = 10 cm, 90 slices, slice thickness = 1mm, scanning time approximately 10 minutes. A modified sampling scheme allowed the sequence to be employed with autocalibration and two-fold undersampling (R=2), thus reducing the imaging time to nearly half of that in the conventional method<sup>22</sup>.

A 3D spoiled gradient echo (SPGR) sequence was used for cartilage morphological measurements (thickness and volume) with the following parameters: TR/TE = 20/6.3, matrix size  $512 \times 512$ , field of view (FOV) = 16cm, locations per slab (LPS) = 100, slice thickness = 1mm, flip angle =  $18^\circ$ .

**T1 $\rho$  and T2 relaxation time mapping**—Sagittal 3D T1 $\rho$ -weighted images were acquired based on spin-lock techniques and 3D SPGR acquisition. Basically, the sagittal 3D T1 $\rho$ -weighted imaging sequence was composed of two parts: magnetization preparation for the imparting of T1 $\rho$  contrast, and an elliptical-centered segmented 3D SPGR acquisition immediately after T1 $\rho$  preparation during transient signal evolution. The duration of the spin-lock pulse was defined as time of spin-lock (TSL), and the strength of the spin-lock pulse was defined as spin-lock frequency (FSL). The number of pulses after each T1 $\rho$  magnetization preparation was defined as views per segment (VPS). There was a relatively long delay (time of recovery, T<sub>rec</sub>) between each magnetization preparation to allow enough and equal recovery of the magnetization before each T1 $\rho$  preparation. The main parameters of this sequence were: FOV=14cm, matrix =  $256 \times 192$ , slice thickness = 3 mm, TR/TE = 9.3/3.7 ms, BW = 31.25 kHz, VPS = 48, T<sub>rec</sub> = 1.5 s, TSL = 0/10/40/80 ms, spin lock frequency = 500 Hz. Sagittal 3D T2 mapping were also acquired by adding a nonselective T2 preparation imaging sequence to the same SPGR sequence as for T1 $\rho$  mapping, with TR/TE = 2000/4.1, 14.5, 25, 45.9 ms. The T2 quantification was acquired subsequently and covered the same regions as the T1 $\rho$  sequence. T1 $\rho$  mapping was assessed in all subjects while only 11 subjects were scanned for T2 mapping.

## Image analysis

The raw data from the conventional accelerated acquisitions as well as the DICOM images were transferred and analyzed on a Sun Workstation (Sun Microsystems, Mountain View, CA). The parallel MRI images acquired with an accelerator factor (AF) of 2 were reconstructed using off-line using GRAPPA based reconstruction routines programmed in MATLAB (MathWorks, Naticks, MA)<sup>25</sup>.

**Trabecular bone processing**—The analysis of trabecular bone structure parameters was then performed using an in-house IDL-based (RSI, Boulder, CO) developed image analysis software<sup>26</sup>. Six different compartments were defined for trabecular bone analysis: femur (F), lateral and medial femoral condyle (LFC/MFC), tibia (T), lateral and medial tibia (LT/MT). These ROIs consisting of trabecular bone and marrow were segmented based on axial images similarly with a previously described processing method<sup>2</sup> as illustrated in Figure 1 and Figure 2.

Based on a dual reference limit and assuming a biphasic model previously described by Majumdar et al.<sup>27, 28</sup>, a global threshold was calculated and bone/marrow binary images were then generated. The structure parameters assessed differ from those derived using histomorphometry, and therefore are considered “apparent” structure parameters. The trabecular structure was evaluated by computing parameters such as apparent bone volume

over total volume fraction - app. BV/TV, apparent trabecular number - app. Tb.N [1/mm], apparent trabecular separation - app. Tb.Sp [mm] and apparent trabecular thickness - app. Tb.Th [mm].

**Cartilage processing**—Cartilage segmentation was performed using an in-house program created with MATLAB (Mathworks, Natick, MA). Based on the sagittal 3D high-resolution SPGR images, the articular cartilage was segmented using a spline-based semi-automatic technique. Four distinct regions were defined: medial (MT) and lateral (LT) tibia, and medial (MFC) and lateral (LFC) femoral condyles. An iterative radius minimization process was implemented for cartilage average thickness and volume computation for each region, as previously described<sup>2</sup>. To account for the variation in joint size, the calculated volume was divided by the epicondylar distance of each respective subject. T1 $\rho$  maps were then reconstructed using a Levenberg-Marquardt mono-exponential in-house developed fitting algorithm. T1 $\rho$ -weighted images intensity obtained for different TSL were fitted pixel-by-pixel to the following equation:  $S(\text{TSL}) \propto \exp(-\text{TSL}/T_{1\rho})$ . Similar to T1 $\rho$  mapping, T2 maps were also generated using the same fitting algorithm applied for the T2-weighted images intensity obtained for different TE:  $S(\text{TE}) \propto \exp(\text{TE}/T_2)$ . Next, the reconstructed T1 $\rho$  and T2 maps were rigidly registered to the previously acquired high-resolution T1-weighted SPGR images using the VTK CISG Registration Toolkit<sup>29</sup>.

### Statistical analysis

All statistical processing was performed with JMP software Version 6 (SAS Institute, Cary, NC). Mean and SD of T1 $\rho$  and T2 values were calculated in each of all these compartments for all the subjects. The coefficients of variation (CV) characterizing the reproducibility of the four bone parameters measurements were assessed on 4 healthy controls based on 2 repeated scans, as previously described<sup>30</sup>. Spearman's rank correlations were performed to correlate bone with cartilage parameters. The comparison between groups as well as to test the variance heterogeneity of the parameters, an analysis of variance ANOVA F-test was performed. For the articular cartilage and trabecular bone parameters that correlated with age, an analysis of covariance (ANCOVA) with adjustment for age was performed for the comparison between patients and controls. P values below 0.05 were considered to denote statistical significance.

## RESULTS

### Subject characteristics

The summary of the characteristics of all subjects is shown in Table 1. A similar number of 16 subjects defined each group. The OA patients had significantly higher age and BMI, whereas the weight was not different between groups. Also, significantly higher values in the WOMAC scores for pain, stiffness and function characterized the OA patients.

### Precision of the MRI measurements

The computed CVs for the trabecular bone structure show good measurement precision (Table 3). Specifically, the CV ranged from 2.4% to 3.7% for app. BV/TV, from 1.8% to 4.1% for app. Tb.N, from 4.1% to 5.5% for app. Tb.Sp and from 1.6% to 4.1% for app. Tb.Th. These results are similar to previous published data at 1.5T<sup>1, 17</sup>. Reproducibility results for the articular cartilage analysis have been previously published<sup>31</sup>.

### Trabecular bone and articular cartilage data

Over all bone and cartilage parameters, the standard deviations are more elevated in OA group due to the heterogeneity of the pathology within OA patients. A comparison between control and OA patient groups in terms of trabecular bone parameters is shown in Figure 4. The articular

cartilage data are plotted in Figure 5 as a comparison between control and OA patient groups. Representative relaxation color maps are illustrated in Figure 3: T1 $\rho$  (A) and T2 (B) maps for a healthy control and T1 $\rho$  (C) and T2 (D) maps for a mild OA patient.

### Correlations between bone structure and cartilage

The Spearman's rank correlations between articular cartilage parameters and bone structure from the same compartment assessed for the mild OA patients group are summarized in Table 4. Correlations between contro-lateral sites of the knee joint were found as well. Thus, MT articular cartilage parameters were highly correlated with all LT trabecular bone parameters. Moderate to weak correlations were also found between MT cartilage parameters and LFC trabecular structure (Table 5). Then LT cartilage parameters were correlated with MFC trabecular bone parameters, as shown in Table 6.

### Correlations between clinical parameters and MRI-based parameters

**a. MRI-based trabecular bone parameters**—Evaluation of the clinical course demonstrated significant correlations between the WOMAC pain score and app. Tb.Sp ( $R^2 = 0.30$ ,  $P=0.043$ ) at the MT as well as app. BV/TV ( $R^2 = -0.36$ ,  $P<0.013$ ) and app. Tb.Th ( $R^2 = -0.37$ ,  $P<0.026$ ) at the T. The WOMAC stiffness was correlated with trabecular structure at the MFC - BV/TV ( $R^2 = -0.31$ ,  $P=0.029$ ), and app. Tb.N ( $R^2 = -0.29$ ,  $P=0.024$ ) - and LFC - app. Tb.Th ( $R^2 = -0.32$ ,  $P=0.025$ ). Few significant correlations were found between bone parameters and the WOMAC function ( $P<0.05$ ).

The patients age also correlated with app. BV/TV ( $R^2 = -0.38$ ,  $P=0.023$ ), app. Tb.Sp ( $R^2 = 0.33$ ,  $P=0.031$ ), and app. Tb.Th ( $R^2 = -0.53$ ,  $P=0.002$ ) at the F, as well as with app. Tb.Th ( $R^2 = -0.34$ ,  $P=0.029$ ) at the LT.

The K-L grade was correlated only with app. Tb.Th at the MFC ( $R^2 = -0.36$ ,  $P=0.037$ ) as well as at the F ( $R^2 = -0.38$ ,  $P=0.021$ ).

**b. MRI-based articular cartilage parameters**—Significant correlations between the three dimensions of the WOMAC score and the articular cartilage parameters were found only at the femur and not at the tibia.

Thus, there was a significant correlation between the WOMAC pain score and the cartilage thickness at the LFC ( $R^2 = 0.44$ ,  $P=0.021$ ), MFC ( $R^2 = 0.40$ ,  $P=0.015$ ) and at the F ( $R^2 = 0.48$ ,  $P=0.011$ ). Also the WOMAC pain score was correlated with T2 values ( $R^2 = 0.39$ ,  $P=0.019$ ) and normalized volume ( $R^2 = 0.34$ ,  $P=0.041$ ) at the LFC. The WOMAC stiffness score was correlated with T1 $\rho$  values in all femoral compartments - LFC ( $R^2 = 0.29$ ,  $P=0.038$ ), MFC ( $R^2 = 0.39$ ,  $P=0.028$ ), and F ( $R^2 = 0.33$ ,  $P=0.045$ ) - as well as with the thickness but only at the F ( $R^2 = 0.40$ ,  $P=0.034$ ). The WOMAC function was correlated with T2 values in all femoral compartments ( $P<0.05$ ).

The patients' age was significantly correlated with T1 $\rho$ , cartilage thickness and normalized volume in all compartments ( $P<0.05$ ), while the T2 values were correlated with patients age only at the MFC ( $R^2 = 0.50$ ,  $P=0.027$ ) and LT ( $R^2 = 0.31$ ,  $P=0.039$ ).

The K-L grade was correlated with T2 values at the MFC ( $R^2 = 0.36$ ,  $P=0.035$ ) and at the femur ( $R^2 = 0.33$ ,  $P=0.043$ ), as well as with the cartilage thickness at the MT ( $R^2 = -0.33$ ,  $P=0.046$ ).

## DISCUSSION

In this study, using high-resolution parallel imaging at 3T, trabecular bone architecture was evaluated in the distal femur and the proximal tibia. An interrelationship between trabecular bone structure and articular cartilage in the knee joint was also demonstrated.

### Parallel imaging

Trabecular bone MRI was conducted with parallel imaging, employing a modified FIESTA-c sequence with autocalibration and two-fold undersampling, which allowed acquisition of 90 slices with an in-plane resolution of  $0.195 \times 0.195 \text{ mm}^2$  within approximately 10 minutes. The same resolution was reported in a previous study<sup>2</sup> done using 1.5T MRI for trabecular bone structure assessment, but the scanning time was approximately twice longer (~19 minutes) for 96 slices acquisition.

### Trabecular bone structure

Trabecular bone structure assessment was characterized by a good reproducibility of the measurements as shown in Table 3. At this early stage of OA, an overall decrease in bone structure parameters found in patients compared with controls. Over all compartments, the app. BV/TV, app. Tb.N, and app. Tb.Th were all typically higher in the femur, and the app. Tb.Sp was lower than in the tibia, consistent with previously published data acquired at 1.5T strength field<sup>1</sup>. Variations in mean bone structure parameters between OA patients and controls indicated that the MR-derived structure measures app. BV/TV and app. Tb.Sp were the most sensitive parameters (Figure 4), with significant difference in all tibial and femoral compartments. Previous studies analyzing the biomechanical strength of trabecular bone structure from spine<sup>32</sup> and knee joint<sup>1</sup> yielded similar findings. Thus, as a result of loading differences and biochemical loads, the structure of trabecular bone is different in the tibia compared with the femur: the bone is denser in femur in general.

### Articular cartilage

In terms of cartilage analysis, at this early stage of OA, a significant increase in T1 $\rho$  and T2 values was found in all femoral compartments, but not at the tibia. Increased values of T1 $\rho$  and T2 relaxation times were also found in OA patients compared with controls. Li et al.<sup>14</sup> reported the relationship between T1 $\rho$  and T2 relaxation times in human OA in an *in vivo* study done at 3T strength field, suggesting that both T1 $\rho$  and T2 increase with the degree of OA, but that T1 $\rho$  has a higher dynamic range for detecting early cartilage degeneration and in consequence is more sensitive than T2.

There were no significant variations in terms of cartilage thickness and normalized volume, so the morphological parameters didn't show significant changes at this early stage of OA. These findings are consistent with those reported by Blumenkrantz et al.<sup>3</sup> who examined the variation of cartilage thickness in individual subjects over 2 years at 1.5T, and showed that the thickness tended to increase after the baseline scan, but decreased substantially by the last scan. They explained that the initial increase of cartilage thickness can be due to the common incidence of cartilage hydration and swelling in early stages of OA.

All the cartilage parameters values for T1 $\rho$  and T2 relaxation times as well as thickness and volume were consistent with previously published data at 3T using both conventional and parallel imaging (AF=2) protocols<sup>31</sup>. The significantly higher values of the T1 $\rho$  and T2 relaxation parameters in OA patients demonstrate initial changes in the cartilage structure compared with the healthy controls.

### Trabecular bone and articular cartilage inter-relationship

Ding et al.<sup>33</sup> revealed that cartilage and bone function as a unit, sustaining together the mechanical forces associated with joint loading and their mechanical properties vary with age, hence these two tissues should be studied and measured in adjunct for understanding OA. The standard deviations over all bone and cartilage parameters were, more elevated in OA group due to the heterogeneity of the pathology within OA patients. Therefore these correlations were only assessed for the mild OA patients group. Negative correlations were found between trabecular bone and cartilage matrix parameters from the same compartment, indicating that deterioration of trabecular bone structure is directly proportional to the increasing values of T1 $\rho$  and T2. Positive correlations were found between trabecular structure and cartilage thickness and volume, suggesting that loss of mineralized trabecular bone is associated with cartilage morphological degradation. The highest correlations were found between articular cartilage parameters from MT and all LT trabecular bone parameters; these similar high correlations were found at 1.5T in a previous study demonstrating a strong interdependence between opposite tibial sites.

Correlations between contro-lateral sides of knee joint were also found, indicating that loss of mineralized trabecular bone on one side of knee joint is related with cartilage loss on the opposite side. This aspect was also previously reported at 1.5T<sup>2, 3</sup>. These studies stated that the association between cartilage changes in one compartment and relative osteopenia in the opposite compartment suggest that slight varus or valgus angular malalignment as result of cartilage degeneration consequently unloads the biomechanical forces in the non-degenerated compartment of the knee. Significant correlations were also found between MRI-based parameters and clinical parameters (WOMAC scores, K-L grade, age). Within these clinical parameters, the strongest correlations were found between all cartilage parameters and patients' age, which should be expected since tissue loss is common as age increased<sup>34</sup>. However, only app. Tb.Th was correlated with the patients' age. Additionally, correlations with K-L grades as well as with WOMAC scores were low to moderate with some of the MRI-based parameters. For example, bone structure loss was correlated with WOMAC pain at the tibia, and with WOMAC function at the femur, whereas increased T1 $\rho$  values were only correlated with WOMAC stiffness in all femoral compartments.

### Potential limitations

A potential criticism of this work may be raised by the fact that the subjects' age and BMI within the control group, which was used as the reference group, were not matched with the one of mild OA group. Given that T1 $\rho$  and T2 parameters are correlated<sup>14</sup>, another limitation of this study could be that some T1 $\rho$  correlations with trabecular bone structure are not also demonstrated by T2. A reason might be the fact that T1 $\rho$  mapping was assessed in all subjects while only 11 subjects were scanned for T2 mapping.

Considering that cartilage degeneration and bone changes are almost inevitable with age, it is difficult to find older, asymptomatic subjects. Similar issues were also noticed and discussed in previous studies<sup>2, 34</sup> reporting that tissue loss is associated with age. The ANCOVA analysis of covariance performed to correct for age (Table 2) confirmed that the age is an essential factor to take into account, considering that OA is an age-dependent disease. A varus/valgus angular malalignment analysis could improve the actual findings which may reveal different aspects of the OA development. However, the main purpose of this study was to determine the interaction or interrelation between the two tissues: articular cartilage and trabecular bone. Despite of these limitations, this work demonstrated significant trends and correlations, and therefore, substantiates the need for further longitudinal studies.



Using MRI based techniques to analyze bone structure only the mineralized portion of bone is measured. The conclusions on the presence or absence of bone cells as the true basis of bone tissue therefore are limited. The loss of mineralized bone may be due to altered biomechanical loading, such as is found in inactivity osteoporosis and non-mineralized bone tissue including bone cells may still persist. Also, the trabecular bone remodeling might be potentially related not only to the mineral metabolism, but also to the metabolism of the organic components of bone trabeculae<sup>35, 36</sup>. These aspects suggest that further study into the role of biochemical markers and their relation to the differences in trabecular architecture between OA knees with minimal or marked cartilage loss is warranted.

## Conclusion

In conclusion, a relationship between trabecular bone structure and articular cartilage from the distal femur and proximal tibia was established. High-resolution 3D MRI performed at 3T strength field using a parallel imaging protocol showed significant improvement in terms of data acquisition and scanning time compared with previous MRI methods. Also, by reflecting early changes in cartilage biochemistry, the cartilage matrix parameters (T1 $\rho$  and T2) might indicate indirect early changes in trabecular bone structure. Furthermore, once the intrinsic connection between bone and cartilage is established, it may be possible to preserve articular cartilage by moderating bone turnover and quality.

These applications, although speculative, emphasizes the potential role of MRI in monitoring the whole knee joint in degenerative joint diseases. These results may be helpful in predicting variations in bone and cartilage, and understanding all these changes may be useful in planning surgical treatments such as corrective osteotomy, and total knee replacements.

## Acknowledgements

**Source of support:** NIH R01 AR46905

## REFERENCES

1. Beuf O, Ghosh S, Newitt DC, Link TM, Steinbach L, Ries M, et al. Magnetic resonance imaging of normal and osteoarthritic trabecular bone structure in the human knee. *Arthritis Rheum* 2002;46:385–393. [PubMed: 11840441]
2. Lindsey CT, Narasimhan A, Adolfo JM, Jin H, Steinbach LS, Link T, et al. Magnetic resonance evaluation of the interrelationship between articular cartilage and trabecular bone of the osteoarthritic knee. *Osteoarthritis Cartilage* 2004;12:86–96. [PubMed: 14723868]
3. Blumenkrantz G, Lindsey CT, Dunn TC, Jin H, Ries MD, Link TM, et al. A pilot, two-year longitudinal study of the interrelationship between trabecular bone and articular cartilage in the osteoarthritic knee. *Osteoarthritis Cartilage* 2004;12:997–1005. [PubMed: 15564067]
4. Buckwalter JA, Mankin HJ. Articular cartilage: degeneration and osteoarthritis, repair regeneration, and transplantation. *Instr Course Lect* 1998;47:487–504. [PubMed: 9571450]
5. Messent EA, Ward RJ, Tonkin CJ, Buckland-Wright C. Tibial cancellous bone changes in patients with knee osteoarthritis. A short-term longitudinal study using Fractal Signature Analysis. *Osteoarthritis Cartilage* 2005;13:463–470. [PubMed: 15922180]
6. Eckstein F, Charles HC, Buck RJ, Kraus VB, Remmers AE, Hudelmaier M, et al. Accuracy and precision of quantitative assessment of cartilage morphology by magnetic resonance imaging at 3.0T. *Arthritis Rheum* 2005;52:3132–3136. [PubMed: 16200592]
7. Dardzinski BJ, Laor T, Schmithorst VJ, Klosterman L, Graham TB. Mapping T2 relaxation time in the pediatric knee: feasibility with a clinical 1.5-T MR imaging system. *Radiology* 2002;225:233–239. [PubMed: 12355010]

8. Mosher TJ, Dardzinski BJ, Smith MB. Human articular cartilage: influence of aging and early symptomatic degeneration on the spatial variation of T2--preliminary findings at 3 T. *Radiology* 2000;214:259–266. [PubMed: 10644134]
9. Dunn TC, Lu Y, Jin H, Ries MD, Majumdar S. T2 relaxation time of cartilage at MR imaging: comparison with severity of knee osteoarthritis. *Radiology* 2004;232:592–598. [PubMed: 15215540]
10. Regatte RR, Akella SV, Borthakur A, Kneeland JB, Reddy R. Proteoglycan depletion-induced changes in transverse relaxation maps of cartilage: comparison of T2 and T1rho. *Acad Radiol* 2002;9:1388–1394. [PubMed: 12553350]
11. Regatte RR, Akella SV, Borthakur A, Kneeland JB, Reddy R. In vivo proton MR three-dimensional T1rho mapping of human articular cartilage: initial experience. *Radiology* 2003;229:269–274. [PubMed: 14519880]
12. Duvvuri U, Reddy R, Patel SD, Kaufman JH, Kneeland JB, Leigh JS. T1rho-relaxation in articular cartilage: effects of enzymatic degradation. *Magn Reson Med* 1997;38:863–867. [PubMed: 9402184]
13. Akella SV, Regatte RR, Gougoutas AJ, Borthakur A, Shapiro EM, Kneeland JB, et al. Proteoglycan-induced changes in T1rho-relaxation of articular cartilage at 4T. *Magn Reson Med* 2001;46:419–423. [PubMed: 11550230]
14. Li X, Benjamin Ma C, Link TM, Castillo DD, Blumenkrantz G, Lozano J, et al. In vivo T(1rho) and T(2) mapping of articular cartilage in osteoarthritis of the knee using 3 T MRI. *Osteoarthritis Cartilage* 2007;15:789–797. [PubMed: 17307365]
15. Wehrli FW, Ford JC, Haddad JG. Osteoporosis: clinical assessment with quantitative MR imaging in diagnosis. *Radiology* 1995;196:631–641. [PubMed: 7644622]
16. Majumdar S. Magnetic resonance imaging of trabecular bone structure. *Top Magn Reson Imaging* 2002;13:323–334. [PubMed: 12464745]
17. Newitt DC, van Rietbergen B, Majumdar S. Processing and analysis of in vivo high-resolution MR images of trabecular bone for longitudinal studies: reproducibility of structural measures and micro-finite element analysis derived mechanical properties. *Osteoporos Int* 2002;13:278–287. [PubMed: 12030542]
18. Vasilic, B.; Ladinsky, GA.; Saha, PK.; Wehrli, FW. *Medical Imaging. San Diego, USA: Proceedings of the International Society for Optical Engineering; 2006. Micro-MRI based image acquisition and processing system for assessing the response to therapeutic intervention.*
19. Lammentausta E, Kiviranta P, Toyras J, Hyttinen MM, Kiviranta I, Nieminen MT, et al. Quantitative MRI of parallel changes of articular cartilage and underlying trabecular bone in degeneration. *Osteoarthritis Cartilage* 2007;15:1149–1157. [PubMed: 17502160]
20. Pruessmann KP, Weiger M, Scheidegger MB, Boesiger P. SENSE: sensitivity encoding for fast MRI. *Magn Reson Med* 1999;42:952–962. [PubMed: 10542355]
21. Sodickson DK, Manning WJ. Simultaneous acquisition of spatial harmonics (SMASH): fast imaging with radiofrequency coil arrays. *Magn Reson Med* 1997;38:591–603. [PubMed: 9324327]
22. Griswold MA, Jakob PM, Heidemann RM, Nittka M, Jellus V, Wang J, et al. Generalized autocalibrating partially parallel acquisitions (GRAPPA). *Magn Reson Med* 2002;47:1202–1210. [PubMed: 12111967]
23. Kellgren JH, Lawrence JS. Radiological assessment of osteo-arthrosis. *Ann Rheum Dis* 1957;16:494–502. [PubMed: 13498604]
24. Bellamy N, Buchanan WW, Goldsmith CH, Campbell J, Stitt LW. Validation study of WOMAC: a health status instrument for measuring clinically important patient relevant outcomes to antirheumatic drug therapy in patients with osteoarthritis of the hip or knee. *J Rheumatol* 1988;15:1833–1840. [PubMed: 3068365]
25. Banerjee S, Choudhury S, Han ET, Brau AC, Morze CV, Vigneron DB, et al. Autocalibrating parallel imaging of in vivo trabecular bone microarchitecture at 3 Tesla. *Magn Reson Med* 2006;56:1075–1084. [PubMed: 17041879]
26. Felson DT, Lawrence RC, Dieppe PA, Hirsch R, Helmick CG, Jordan JM, et al. Osteoarthritis: new insights. Part 1: the disease and its risk factors. *Ann Intern Med* 2000;133:635–646. [PubMed: 11033593]
27. Majumdar S, Genant HK. A review of the recent advances in magnetic resonance imaging in the assessment of osteoporosis. *Osteoporos Int* 1995;5:79–92. [PubMed: 7599453]

28. Majumdar S, Newitt D, Jergas M, Gies A, Chiu E, Osman D, et al. Evaluation of technical factors affecting the quantification of trabecular bone structure using magnetic resonance imaging. *Bone* 1995;17:417–430. [PubMed: 8573417]
29. Rueckert D, Sonoda LI, Hayes C, Hill DL, Leach MO, Hawkes DJ. Nonrigid registration using free-form deformations: application to breast MR images. *IEEE Trans Med Imaging* 1999;18:712–721. [PubMed: 10534053]
30. Gluer CC, Blake G, Lu Y, Blunt BA, Jergas M, Genant HK. Accurate assessment of precision errors: how to measure the reproducibility of bone densitometry techniques. *Osteoporos Int* 1995;5:262–270. [PubMed: 7492865]
31. Zuo J, Li X, Banerjee S, Han E, Majumdar S. Parallel imaging of knee cartilage at 3 Tesla. *J Magn Reson Imaging* 2007;26:1001–1009. [PubMed: 17896394]
32. Link TM, Majumdar S, Lin JC, Newitt D, Augat P, Ouyang X, et al. A comparative study of trabecular bone properties in the spine and femur using high resolution MRI and CT. *J Bone Miner Res* 1998;13:122–132. [PubMed: 9443798]
33. Ding M, Dalstra M, Linde F, Hvid I. Mechanical properties of the normal human tibial cartilage-bone complex in relation to age. *Clin Biomech (Bristol, Avon)* 1998;13:351–358.
34. Yamada K, Healey R, Amiel D, Lotz M, Coutts R. Subchondral bone of the human knee joint in aging and osteoarthritis. *Osteoarthritis Cartilage* 2002;10:360–369. [PubMed: 12027537]
35. Lajeunesse D, Reboul P. Subchondral bone in osteoarthritis: a biologic link with articular cartilage leading to abnormal remodeling. *Curr Opin Rheumatol* 2003;15:628–633. [PubMed: 12960492]
36. Buckland-Wright JC, Messent EA, Bingham CO 3rd, Ward RJ, Tonkin C. A 2 yr longitudinal radiographic study examining the effect of a bisphosphonate (risedronate) upon subchondral bone loss in osteoarthritic knee patients. *Rheumatology (Oxford)* 2007;46:257–264. [PubMed: 16837470]

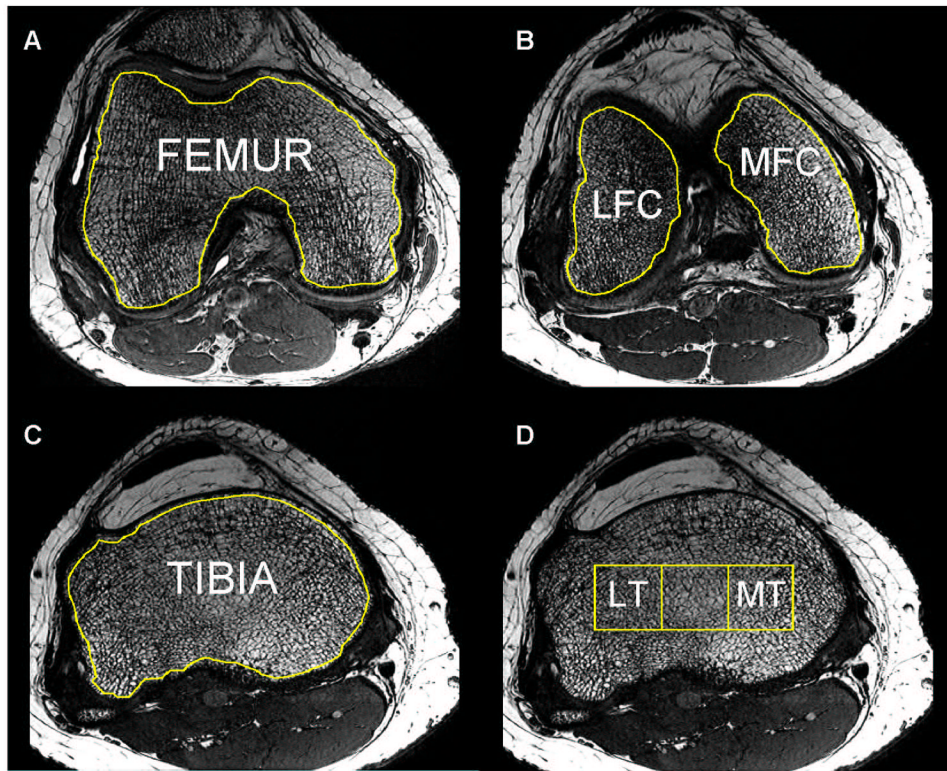


**Figure 1.** Trabecular bone structure post-processing: bone and marrow regions of interest (ROI) were outlined for the femur (A), lateral and medial condyles (B), tibia (C) and lateral and medial tibia (D); the tibial grid was derived from the epicondylar distance (Unit [mm] = Epicondylar Distance  $\times$  100/9).

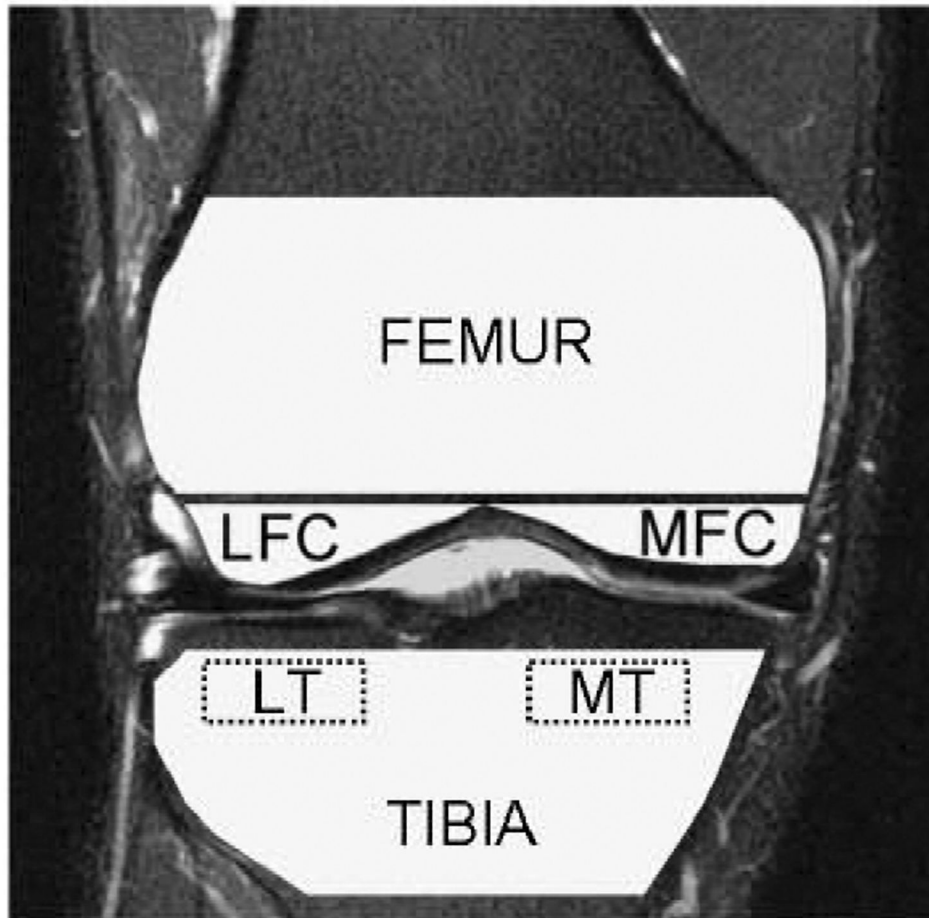


**Figure 2.**

A graphical representation of the segmented trabecular bone regions. The femur, tibia, lateral femoral condyle (LFC), medial femoral condyle (MFC), lateral tibia (LT), and medial tibia (MT) are shown; the ROIs were defined similarly with a previous described method<sup>2</sup>

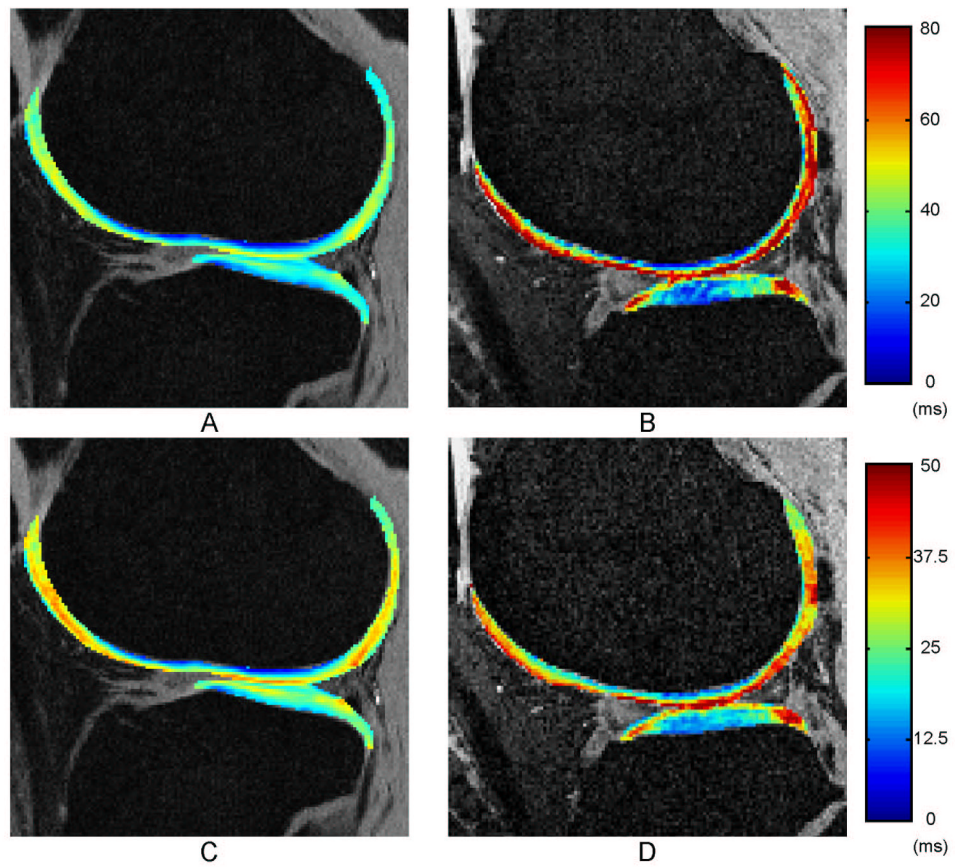


**Figure 3.** Representative T1 $\rho$  and T2 maps for a control subject (A, C) and for an OA patient (B, D).

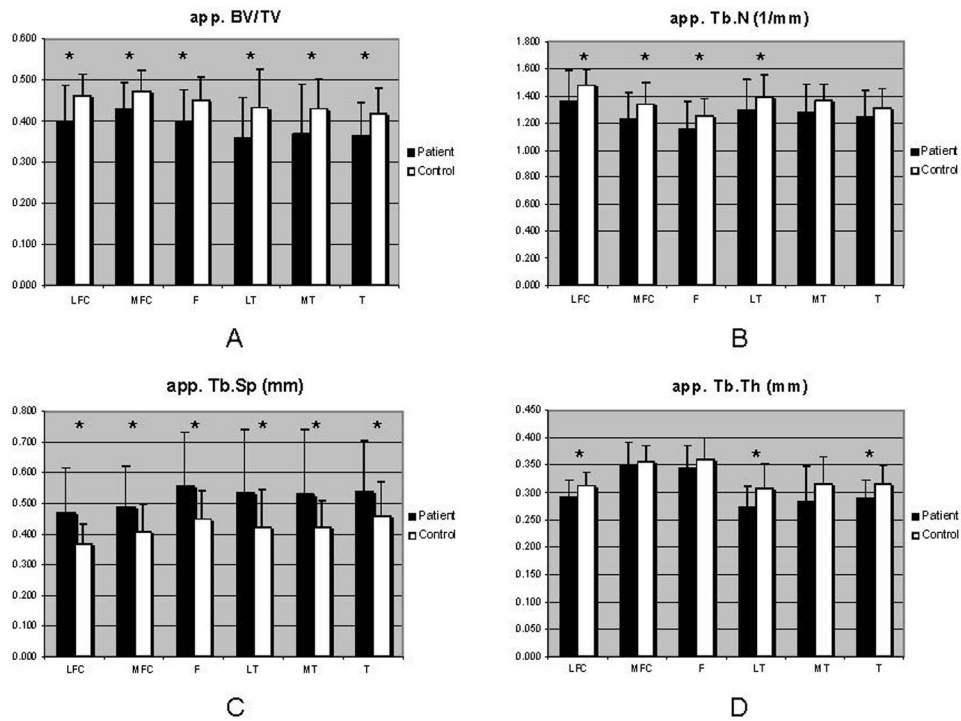


**Figure 4.** Trabecular bone structure data: apparent measures of trabecular bone fraction (BV/TV), trabecular number (Tb.N), trabecular separation (Tb.Sp), and trabecular thickness (Tb.Th) were computed in OA patients compared with controls, using the ANOVA F-test; \*P<0.05.

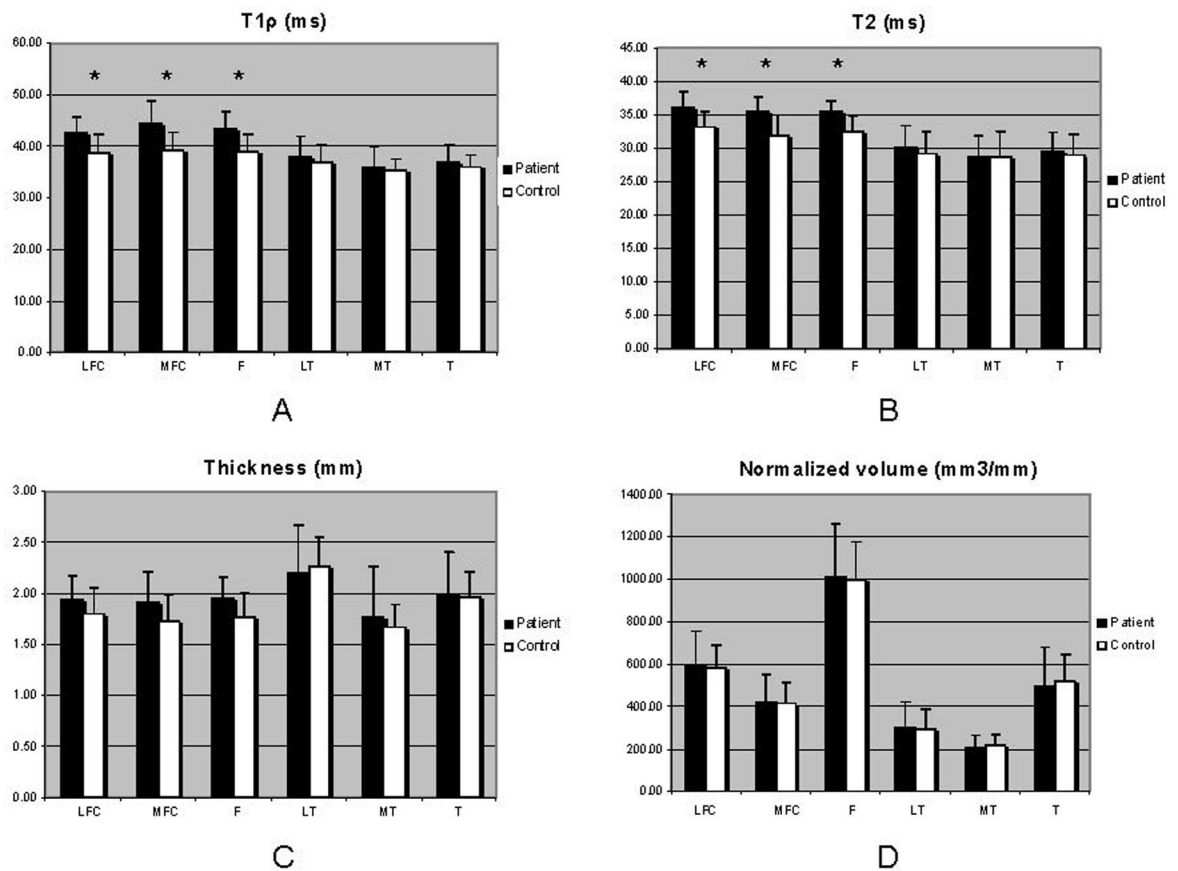


**Figure 5.** Articular cartilage data: T1ρ and T2 relaxation times as well as thickness and normalized volume were computed in OA patients compared with controls, using the ANOVA F-test; to account for the variation in joint size, the calculated volume was normalized to the epicondylar distance of each respective subject; the epicondylar distance was used to standardize the volume due to its invariance to osteoarthritic changes; \*P<0.05.



**Table 1**

Summary of subject characteristics: age, weight and BMI values as well as WOMAC OA parameters are reported as means  $\pm$  SD. Kellgren-Lawrence grades are also shown. P values indicate the significance level of differences between patients and controls.

	Patients	Controls	P-values
Study population [n]	16	16	
Age [years]	47.19 $\pm$ 11.54	36.25 $\pm$ 10.54	0.009
Weight [kg]	80.08 $\pm$ 17.70	70.44 $\pm$ 11.84	0.080
BMI	26.78 $\pm$ 4.83	22.64 $\pm$ 3.03	0.007
<i>Kellgren-Lawrence grade [n]</i>			
Grade	0	16	
Grade 1	7	0	
Grade 2	9	0	
<i>WOMAC OA index</i>			
Pain	5.31 $\pm$ 2.63	1.94 $\pm$ 2.95	0.002
Stiffness	3.25 $\pm$ 1.24	0.63 $\pm$ 0.93	<0.0001
Function	15.06 $\pm$ 7.60	2.81 $\pm$ 6.57	<0.0001

Mean and standard deviations (SD) of articular cartilage and trabecular bone parameters that correlated with age: comparison between patients and controls without (ANOVA) and with adjustment for age (ANCOVA); P values below 0.05 were considered to denote statistical significance.

**Table 2**

Parameters	Compartment	Patients		Controls		Statistical raw		Significance Adjusted for age	
		Mean ± SD		Mean ± SD		P value		P value	
AGE		47.19 ± 11.54		36.25 ± 10.54		0.009			
app. BV/TV	F	0.397 ± 0.08		0.449 ± 0.06		0.011		0.024	
app. Tb.Sp	F	0.557 ± 0.17		0.450 ± 0.09		0.019		0.035	
app. Tb.Th	LT	0.272 ± 0.04		0.308 ± 0.05		0.010		0.020	
Tirho	LFC	42.83 ± 2.95		38.81 ± 3.56		0.004		0.030	
Tirho	MFC	44.44 ± 4.30		39.15 ± 3.49		0.005		0.007	
Tirho	F	43.37 ± 3.38		38.98 ± 3.25		0.004		0.011	
T2	MFC	35.5 ± 2.23		31.89 ± 3.09		0.003		0.022	

**Table 3**

Reproducibility of bone structure measurements: coefficients of variation (CV) of bone parameters measurements on 4 healthy controls based on 2 repeated scans; mean, standard deviation (SD) and standard error of mean (S.E.M.) are also reported.

	FEMUR				LATERAL FEMORAL CONDYLE				MEDIAL FEMORAL CONDYLE			
	BV/TV	Tb.N	Tb.Sp	Tb.Th	BV/TV	Tb.N	Tb.Sp	Tb.Th	BV/TV	Tb.N	Tb.Sp	Tb.Th
MEAN	0.483	1.323	0.393	0.367	0.487	1.544	0.333	0.318	0.503	1.385	0.361	0.367
SEM	0.008	0.056	0.014	0.020	0.010	0.046	0.016	0.007	0.008	0.052	0.014	0.015
SD	0.015	0.113	0.028	0.039	0.019	0.093	0.033	0.013	0.016	0.104	0.028	0.031
CV	<b>0.031</b>	<b>0.019</b>	<b>0.041</b>	<b>0.024</b>	<b>0.042</b>	<b>0.026</b>	<b>0.055</b>	<b>0.036</b>	<b>0.024</b>	<b>0.032</b>	<b>0.048</b>	<b>0.032</b>
	TIBIA				LATERAL TIBIA				MEDIAL TIBIA			
	BV/TV	Tb.N	Tb.Sp	Tb.Th	BV/TV	Tb.N	Tb.Sp	Tb.Th	BV/TV	Tb.N	Tb.Sp	Tb.Th
MEAN	0.454	1.401	0.393	0.325	0.433	1.502	0.392	0.308	0.482	1.428	0.363	0.341
SEM	0.010	0.064	0.022	0.014	0.029	0.076	0.047	0.014	0.034	0.054	0.021	0.034
SD	0.019	0.128	0.044	0.029	0.057	0.152	0.093	0.028	0.068	0.108	0.041	0.068
CV	<b>0.037</b>	<b>0.021</b>	<b>0.053</b>	<b>0.016</b>	<b>0.034</b>	<b>0.037</b>	<b>0.043</b>	<b>0.023</b>	<b>0.037</b>	<b>0.018</b>	<b>0.042</b>	<b>0.041</b>

NOTE: All trabecular bone parameters are "apparent" parameters – app. BV/TV, app. Tb.N, app. Tb.S, app. Tb.Th.

**Table 4**

Spearman's rank correlations between articular cartilage and trabecular structure parameters within the same compartment.

	LATERAL FEMORAL CONDYLE				MEDIAL FEMORAL CONDYLE				FEMUR			
	BV/TV	Tb.N	Tb.Sp	Tb.Th	BV/TV	Tb.N	Tb.Sp	Tb.Th	BV/TV	Tb.N	Tb.Sp	Tb.Th
<b>TIp (n=16)</b>	-0.31*	-0.24*	0.33*	-0.28*	-0.29*	-0.34*	0.36*	NS	-0.26*	-0.31*	0.39*	NS
<b>T2 (n=11)</b>	NS	NS	NS	NS	NS	NS	NS	NS	NS	NS	NS	0.35*
<b>Thickness</b>	NS	NS	NS	NS	NS	NS	NS	NS	0.33*	NS	NS	0.46**
<b>Normalized volume</b>	NS	NS	NS	NS	NS	0.52***	-0.41**	NS	0.30*	0.30*	-0.35*	NS

	LATERAL TIBIA				MEDIAL TIBIA				TIBIA			
	BV/TV	Tb.N	Tb.Sp	Tb.Th	BV/TV	Tb.N	Tb.Sp	Tb.Th	BV/TV	Tb.N	Tb.Sp	Tb.Th
<b>TIp (n=16)</b>	-0.60***	-0.61***	0.64**	-0.46**	NS	NS	NS	NS	-0.44**	-0.30*	0.47**	-0.43**
<b>T2 (n=11)</b>	-0.59**	-0.70**	0.71***	-0.40**	NS	NS	NS	NS	-0.41**	-0.57**	0.56**	NS
<b>Thickness</b>	0.47**	0.32*	-0.35*	0.52**	0.32	NS	NS	0.42**	0.34*	NS	NS	0.32*
<b>Normalized volume</b>	0.68***	0.51**	-0.50**	0.66***	NS	NS	NS	NS	0.44**	0.45***	-0.41**	0.27*

\* P<0.05

\*\* P<0.01

\*\*\* P<0.001

NS = Not Significant

NOTE: All trabecular bone parameters are "apparent" parameters – app. BV/TV, app. Tb.N, app. Tb.S, app. Tb.Th.

Spearman's rank correlations between medial tibia (MT) cartilage parameters and lateral femoral condyle (LFC) and lateral tibia (LT) bone structure.

**Table 5**

MT cartilage parameters	LFC bone parameters			LT bone parameters		
	app. BV/TV	app. Tb.N	app. Tb.Sp	app. Tb.Th	app. Tb.N	app. Tb.Th
T1ρ (n=16)	-0.54**	-0.45**	0.51**	-0.48*	-0.57**	0.57**
T2 (n=11)	NS	NS	NS	NS	-0.65***	0.62***
Thickness	NS	NS	NS	0.30*	0.28*	-0.35*
Normalized volume	NS	0.34*	NS	NS	0.54**	-0.51**

\* P<0.05

\*\* P<0.01

\*\*\* P<0.001

NS = Not Significant.

**Table 6**

Spearman's rank correlations between lateral tibia (LT) cartilage parameters and medial femoral condyle (MFC) bone structure.

MFC bone parameters	LT cartilage parameters			
	T1ρ (n=16)	T2 (n=11)	Thickness	Normalized volume
app. BV/TV	NS	NS	NS	NS
app. Tb.N	-0.42**	-0.41*	0.29*	0.39*
app. Tb.Sp	0.35*	0.32*	NS	-0.30*
app. Tb.Th	-0.40*	NS	0.33*	0.39*

\* P<0.05

\*\* P<0.01

NS = Not Significant.